Springer

KSME

Journal of Mechanical Science and Technology 24 (10) (2010) 2043~2050
www.springerlink.com/content/1738-494x
DOI 10.1007/s12206-010-0621-z

Experimental studies on the flow characteristics in an oscillating water column device †

Krishnil Ram[1], Mohammed Faizal[1], M. Rafiuddin Ahmed[1] and Young-Ho Lee[2,*]

[1]*Division of Mechanical Engineering, The University of the South Pacific, Laucala Campus, Suva, Fiji*
[2]*Division of Mechanical and Information Engineering, Korea Maritime University, 1 Dongsam-dong Youngdo-Ku, Busan 606-791, Korea*

(Manuscript Received January 6, 2010; Revised June 1, 2010; Accepted June 15, 2010)

Abstract

A fixed type oscillating water column (OWC) device was designed and tested in a 2-D wave channel. The air chamber was converged to its minimum area at the turbine section to obtain the maximum kinetic energy. The variations in the height of water in the water column and in the static pressure of the air caused by the oscillating waves were studied in detail. The airflow in the entire air chamber was documented with particle image velocimetry measurements. No turbine was installed in the device. The experiments were performed by varying the water depth and the wave frequency. It was found that the air velocities in the turbine chamber during the upward motion of water in the column are always larger than during the downward motion. While the airflow was strong most of the time, very low air velocities were recorded during the transition between the upward and downward flows indicating the need of an airflow regulator before the turbine to get a constant flow rate of air. The well-directed flow obtained at the turbine section can be used to drive a Savonius rotor, which is the most appropriate turbine for rectangular cross-section of the chamber.

Keywords: Wave energy; Oscillating water column; Particle image velocimetry experiments

1. Introduction

Water waves are always present on the ocean surface as long as there is wind blowing over the ocean, thus offering an infinite source of wave energy. The power flow in the waves is up to five times compared to the wind that generates the waves, making wave energy more persistent than wind energy [1]. The common factors that determine the characteristics of the wind-generated waves are the wind velocity, the distance over which the wind is in contact with the sea and for how long they are in contact [2]. Water wave motions are complex and irregular on the ocean surface. Mathematical analysis becomes easier when idealized solutions are considered. Experimentally, it is convenient to study two-dimensional waves in channels with parallel side-walls. Regular sinusoidal waves [3-5] are easier to study compared to non-linear waves. The effects of boundary layer are very small and can be neglected [6]. Common parameters of a sinusoidal wave are the wave period (T), the wavelength (L), and the wave height (H).

Modern instrumentation allow accurate measurement of wave parameters. Particle image velocimetry (PIV) is now a standard optical method for instantaneous mapping of flow fields and can measure particle velocities over a large 2-D area of a flow field [7]. The flow is seeded with particles, which are illuminated and their positions recorded photographically [8, 9].

Surface water waves have energy associated with them - kinetic energy of the moving particles and potential energy due to the vertical position of water. The total wave energy is proportional to the square of the wave height and is equally divided between kinetic and potential energies [5, 6]. A number of devices are now developed to extract energy from the waves [1, 2]. Wave energy is attracting a lot of attention now, as it is available 90% of the time at a given site compared to solar and wind energies which are available 20-30% of the time [10]. According to McCormick [2], there are some basic concepts on which wave energy extraction devices are based. Heaving and pitching bodies make use of the surface displacement of water as an energy source. Pressure devices utilize the hydrostatic and dynamic pressure changes beneath the water waves. Surging wave energy converters capture wave energy as waves enter the surf zone. Cavity resonators make use of the displacement of water in a water column. Particle motion converters obtain energy from the moving water particles.

Oscillating water column (OWC) wave energy converters

† This paper was recommended for publication in revised form by Associate Editor Jun Sang Park

*Corresponding author. Tel.: +82 51 410 4293, Fax: +82 51 403 0381
E-mail address: lyh@hhu.ac.kr

are similar to cavity resonators because they use water columns to convert energy. Shoreline OWC wave energy converters have attracted a lot of attention because of their simple operation. The waves act like a giant reciprocating piston compressing and de-compressing the trapped air. OWC wave energy converters are partly submerged devices; the submerged structure partially encloses a column of water open to the incident waves through the opening in the lower part of the device. As the waves impinge on the device, the internal free surface of the water column undergoes oscillatory motion. The alternating flow compresses and expands the inner mass of the air that is trapped in the chamber. The induced bi-directional airflow can be used to drive an air turbine. A good design of an OWC wave energy converter requires a thorough understanding of the airflow characteristics in the air chamber, as the reciprocating air affects the performance of the OWC converter. A number of numerical and experimental studies have been performed on OWC devices [11-17]. Evans and Porter [11] used a pressure distribution model to obtain the hydrodynamic coefficients of an OWC device. Delauré and Lewis [12] performed a parametric study of an OWC system with the help of 3-D low order panel method. Josset and Clément [13] employed a hybrid method from time-domain simulation of OWC wave power plants. The simulation of the movements of the inner free surface due to the excitation of the outer-sea waves was split into two sub-problems: an outer one, dealing with the incident, diffracted and radiated waves, and an inner one, concerning the inner water volume behavior. Conde and Gato [14] performed a numerical study of the airflow in a typical pneumatic chamber of an OWC type wave energy converter. They performed calculations to investigate the flow distribution at the turbines' inlet sections, as well as the properties of the air-jet impinging on the water free-surface. Falcão and Justino [15] theoretically analyzed the performance of an OWC wave energy device when two types of valves – a bypass valve mounted in parallel with the turbine or a valve mounted in the turbine duct – to prevent the flow rate through the turbine from becoming excessive. Sarmento [16] performed experiments on an OWC in a wave flume with regular waves of small amplitude-to-wavelength ratio. The measurements showed that the amount of energy radiated by higher-order waves (resulting from nonlinearity) was very small and did not prevent the maximum efficiency from being reached, close to the values achievable in the linear case. Koola et al. [17] performed experiments on a scaled-down model in a 300 mm wide wave flume at a mean water depth of 120 mm and a significant wave height of 15.2 mm. They varied the OWC's side-wall thickness, lip thickness and wave frequency. They found that thicker walls with rounded edges enhance energy absorption capability. They also found that the performance of the model peaked at $f = 0.9$ Hz. There have also been numerous research efforts directed at designing a suitable turbine to extract power from the fluctuating flow of air in the OWC's air chamber. A review of the different impulse turbines developed for energy extraction from OWC devices is performed by Setoguchi et al. [18]. The airflow in the OWC's air column is known to be oscillating and complex. The efficiency of oscillating water column (OWC) wave energy devices equipped with Wells turbines is particularly affected by flow oscillations basically for two reasons: 1) due to the intrinsically unsteady (reciprocating) flow of air displaced by the oscillating water free surface, and 2) increasing the airflow rate above a limit depending on and approximately proportional to the rotational speed of the turbine is known to give rise to a rapid drop in the aerodynamic efficiency and in the power output of the turbine [15]. Conventional turbines such as Wells turbine are also expensive to develop and maintain for wave energy plants. Of late, there is a growing interest in rectangular OWC chambers and rectangular turbine sections housing Savonius rotors [19, 20]. The advantage lies in the ease of construction of these types of turbines as well as the OWC; it also allows us to increase the width of OWC parallel to the coast so that a greater amount of energy can be absorbed per device. Unlike the circular OWC, the width of entry of the capture chamber can be increased in the rectangular ducted OWC without being influenced by the diameter at the turbine section. The Savonius turbine is much cheaper and is an effective option at low Reynolds numbers, unlike the Wells turbine which requires a high Reynolds number [20]. Menet [21] remarks that their high starting torque not only allows them to run but also start whatever the wind speed. The generation unit where the conversion of energy takes place can be placed at the surface. In case of OWCs, this provides ease of maintenance. It cannot be ignored that Savonius rotors have lower efficiencies than horizontal axis turbines for wind applications. However, in the case of OWCs, the simplicity of the Savonius along with its other advantages make it a competitive option as a power producing turbine. In 2008, Altan and Atılgan [22] proposed the idea of a curtain placed in front of a Savonius wind rotor to increase its performance. The curtain causes air to be channeled onto the inner blades rather than impacting the outer portion of the adjacent blade. This reduces negative torque in the Savonius rotor. A novel approach of incorporating the curtain effect into the chamber of the OWC is presented in the present work. The contracting curtains need to be placed on both sides of the turbine due to bi-directional flow. Setoguchi and Takao [23] highlight that the efficiency of the turbine does not provide useful information about the suitability of the turbine for wave power conversion. This is because the turbine characteristics depend on the efficiency of the air chamber , i.e the ratio of the OWC and the incident wave power. Hence it is desirable that the primary conversion process be as much efficient as practically possible to ensure optimum energy conversion rate of the overall OWC. The present work is aimed at experimentally studying the airflow characteristics through the air chamber and the turbine chamber of a rectangular OWC device in a two-dimensional (2-D) wave channel. The paper details the airflow characteristics through this newly designed capture chamber, which shows some promising results.

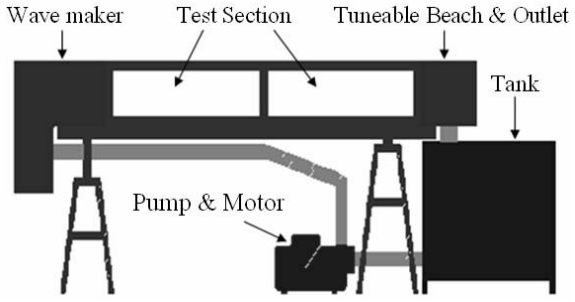

Fig. 1. Schematic diagram of the wave channel.

2. Experimental set-up and procedure

The experiments were carried out in a *Cussons* Wave Channel, model P6325, available in the Thermo-fluids laboratory of the University of the South Pacific. The wave channel has a length of 3500 mm, a width of 300 mm and a depth of 450 mm. The side walls are made of Plexiglas to allow a clear view of the wave action. A flap type wave maker, hinged at the bottom, produces oscillatory, sinusoidal waves. A frequency range of 0 to 1.4 Hz can be set. The close fit of the wave maker to the channel sides ensures that 2-D waves are produced with no fluid motion normal to the sidewalls [7, 24]. The water flow is generated by a centrifugal pump having a rated capacity of 40 Lit/s at a total head of 10 m and is driven by a 5.5 kW motor. The pump draws water from a tank, as shown in Fig. 1. To minimize reflection of the waves, a *Cussons* Tuneable Beach, model P6285, was installed at the end of the wave channel. It employs a series of porous plates with different porosity levels to absorb the wave energy gradually. The use of different plates with a variable spacing between them allowed a wide variety of wave profiles to be absorbed.

A schematic diagram of the OWC device is shown in Fig. 2. The air chamber was converged from an initial cross-sectional area of 290 mm × 80 mm to its minimum area of 80 mm × 80 mm at the turbine section to obtain maximum kinetic energy. The inner surface of the sharp edges on either side of the turbine chamber was smoothened with the help of silicone sealant to provide a smooth flow and prevent any recirculation in that region. It is expected that a clockwise-rotating turbine will receive all the flow entering from both the sides of this section, and the two corners will not affect the performance of the turbine. The exit of the chamber is a diffuser which serves as a link to the atmosphere. For pressure measurements, five pressure taps were provided on the rear wall of the air chamber at different locations, as shown in Fig. 2.

The pressure measurements in the air chamber were performed with a FCO510 digital Micromanometer connected to a PC through RS232. The wave height and the wavelength were measured using *Seiki* pressure transducers, model PSHF002KAAG; the data were acquired on a GL500A midiOGGER dual datalogger.

The wave frequency (f) and the water depth (D) were varied from 0.58 Hz to 1.1 Hz and 240 mm to 300 mm respectively

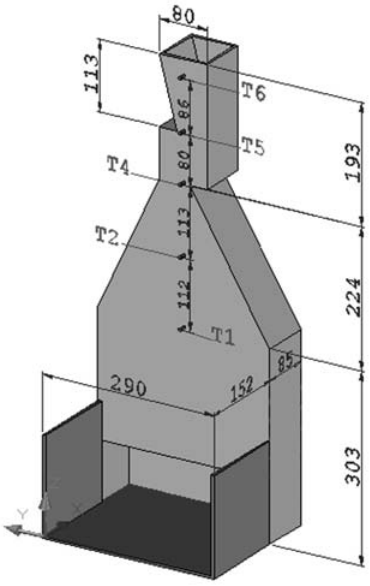

Fig. 2. Schematic diagram of the OWC device.

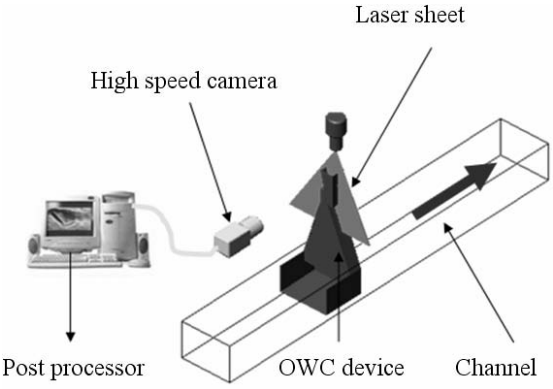

Fig. 3. Schematic diagram of the PIV set-up.

in these experiments. The distance of the OWC device from the paddle was kept much greater than twice the depth of the hinge to ensure fully developed waves [24].

The PIV system used in the present studies consisted of a 500 mW air-cooled Diode-Pumped Solid State continuous light laser and a high-speed *Photron* CCD camera. The 532 nm output of the laser was converted to a laser sheet and delivered to the desired location. Olive oil was atomized to particles of average diameter 1 μm and injected into the flow for seeding. The camera recorded 500 frames per second, producing up to 1280 x 1024 pixel images. The images captured by the CCD camera were processed using *Cactus 3.3* software. Fig. 3 shows the PIV set-up and the wave channel. The wave period was measured by recording the time taken for two successive crests to pass a given point. The factors which were considered for determining the accuracy of velocity measurements with PIV are: the uncertainties due to finite time sampling, finite displacement of the particles, and uncertainties in measuring the displacements of the particle images [9]. The

accuracy of displacement measurements with *Cactus* is of the order of 0.1 pixel. For the high speed camera, the time resolution for the current measurements was 0.008 s. To get an accurate estimate of the uncertainty in our measurements, PIV measurements were performed on a calibrated, constant speed rotating motion and the maximum error was found to be 0.32%.

3. Results and discussion

Fig. 4 shows the variations of the wavelength with frequency for different depths. It can be seen that the wavelength reduces with increasing frequency. It is interesting to note that the wavelengths are lower for greater mean water depths. For the maximum mean water depth of 300 mm, the wavelengths are found to be the smallest.

The variation of the wave height with frequency at different depths can be seen in Fig. 5. It is clear that the wave height increases with frequency. Even in ocean waves, L and H are inversely proportional. The wave heights are higher for greater depths and the maximum wave heights are recorded at the maximum depth of 300 mm, indicating that the energy transfer from the wave-maker to the water is maximum at the maximum depth due to the maximum area of contact between the flap and water. The wave energy is proportional to the square of wave height, as discussed earlier [5, 6], which is the highest at the maximum depth of 300 mm.

The variations in the height of the water column inside the chamber about the mean level for the frequencies of 0.6, 0.7, 0.8, 0.9 and 1.0 Hz are shown in Fig. 6. The data were acquired every second (averaged over one second) for a duration of initial 8 seconds. The data acquisition was stopped when the reflections of the waves from the OWC start affecting the incoming waves. The variations are small at the frequency of 0.6 Hz, as expected.

The fluctuations in the water level in the OWC are higher at the frequency of 0.7 Hz compared to 0.6 Hz. For the case of f = 0.8 Hz, it was found that the fluctuations reduce compared to the lower frequencies. It can also be seen that the rise and drop in the water level reduce with time, which is apparently due to the onset of interference because of the wave breaking effects of the OWC itself. Very interesting observations were made for the higher frequencies of 0.9 and 1.0 Hz. For f = 0.9 Hz, the fluctuations were consistent and did not change with time like other frequencies, whereas for f = 1.0 Hz, the fluctuations increased gradually with time. The maximum fluctuations were recorded at this frequency. Further experiments revealed that wave breaking starts at this frequency. As the fluctuations were consistent and the energy is the highest at f = 0.9 Hz compared to lower frequencies, most of the experiments were performed at this frequency.

The results of the pressure measurements at the five taps for two depths of 260 mm and 290 mm at a frequency of 0.9 Hz are shown in Figs. 7 and 8 respectively. The data were acquired every 300 ms for a duration of 8 seconds for the same

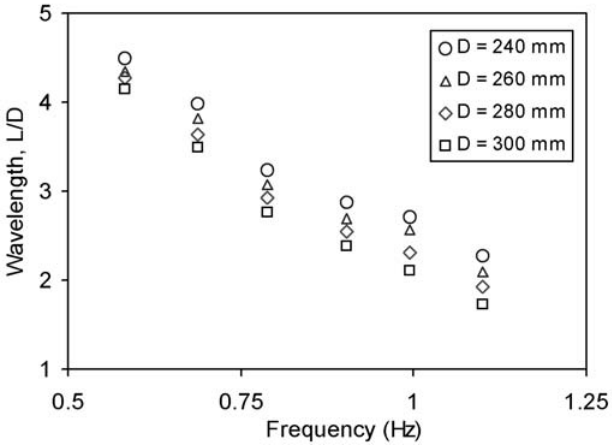

Fig. 4. Variation of the wavelength with frequency at different depths.

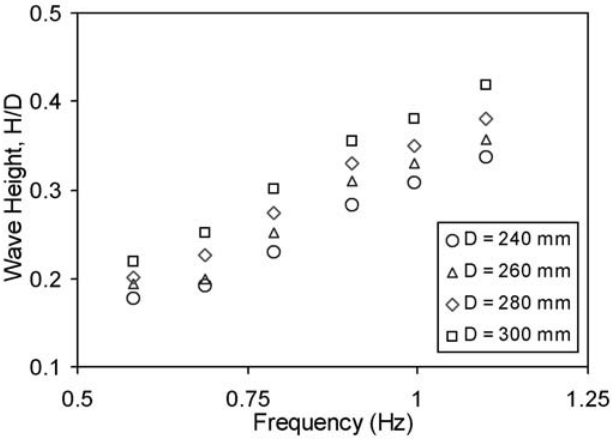

Fig. 5. Variation of the wave height with frequency at different depths.

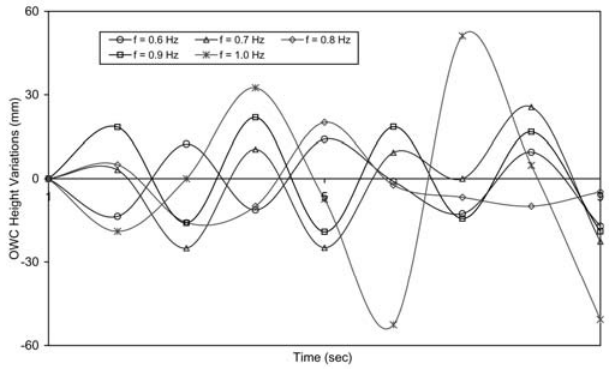

Fig. 6. Variations in the OWC height with time.

reason mentioned above. The experiments on the pressure measurements were repeated many times and a very large number of data sets were acquired to obtain accurate values of static pressures at the five pressure taps. It is interesting to note that the peak suction at all the points is always higher than the positive pressure at those points. At taps 1 and 2, where the flow area is larger and the velocities are small, both the suction and positive pressures are found to be large. As the

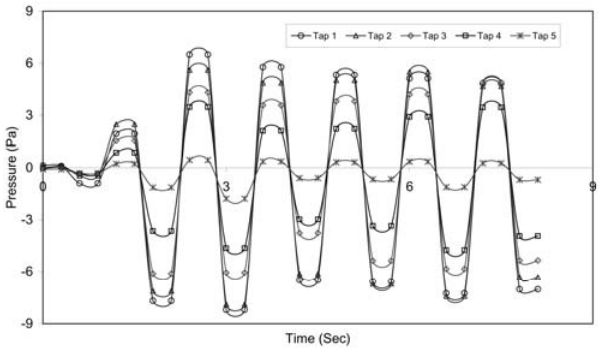

Fig. 7. Variations of wall static pressure at the five pressure taps with time at f = 0.9 Hz for D = 260 mm.

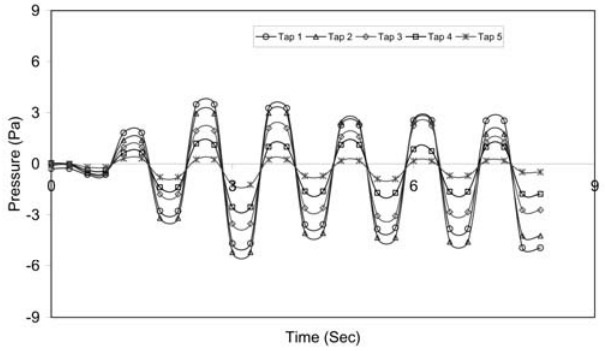

Fig. 8. Variation of wall static pressure at the five pressure taps with time at f = 0.9 Hz for D = 290 mm.

area reduces, the air velocity increases at the expense of the static pressure. At the last pressure tap (tap 5) that was located at about 25 mm from the exit of the air chamber, both the positive and suction pressures are found to be minimum for all the depths.

Both the positive and suction pressures at all the pressure taps were found to increase slightly with increasing depth till the maximum depth of 300 mm indicating that the higher fluctuations in the water column are resulting in higher air velocities in the air chamber in both the directions with increasing depth. The higher velocities are indicative of higher kinetic energy of the air available to drive the turbine.

The velocity measurements with PIV were performed in the air chamber focusing on the turbine chamber (between taps 3 and 4 in Fig. 2) as well as on the entire air chamber to gain a better understanding of the airflow pattern. It was found that the airflow velocities and the available power are the highest at the frequency of 0.9 Hz due to higher and consistent fluctuations in water column (Fig. 6) providing a consistent driving force for the airflow. Fig. 9 shows the vectors of the resultant velocity in the turbine chamber during the upward motion of the air (as a result of wave impingement). It can be seen that there is a strong upward flow of the air in the turbine chamber that is slightly inclined towards the left. From Fig. 2, it is clear that the leftward motion is a result of the contraction design which directs the flow towards the left. Such a directed

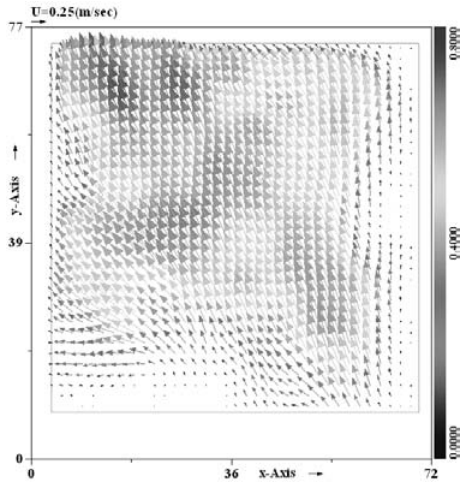

Fig. 9. Velocity vectors showing the airflow during the upward motion at f = 0.9 Hz for D = 260 mm.

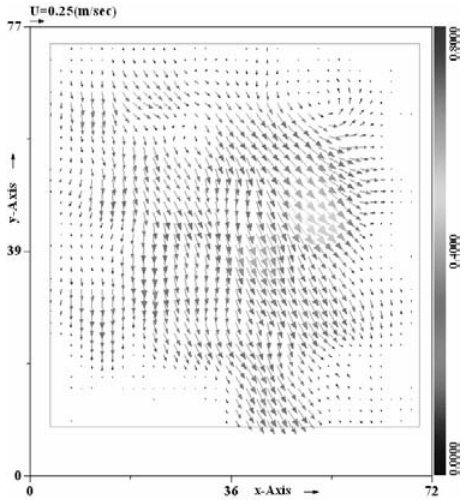

Fig. 10. Velocity vectors showing the airflow during the downward motion at f = 0.9 Hz for D = 260 mm.

flow will impart a higher momentum to the blades of the Savonius rotor turbine that will be designed to rotate in the clockwise direction. It is also observed from the detailed PIV measurements that the flow is accelerating at the exit of the contraction nozzle because it has a consistently reducing area.

The downward airflow through the turbine chamber is similarly inclined to the right, as shown in Fig. 10, and will impart energy to the turbine rotating in the clockwise direction. As discussed earlier, it is expected that most of the converged flow will be received by the turbine blades. While the downward flow of air during the suction (downward motion of water in the chamber) is also strong most of the time, the air velocities during the downward flow are lower compared to those during the upward flow, as can be seen from a comparison of Figs. 9 and 10. This is supported by the fact that the positive pressures felt at the five pressure taps are lower (indicating higher upward velocities) compared to the negative pressures (indicating lower downward velocities), as shown in

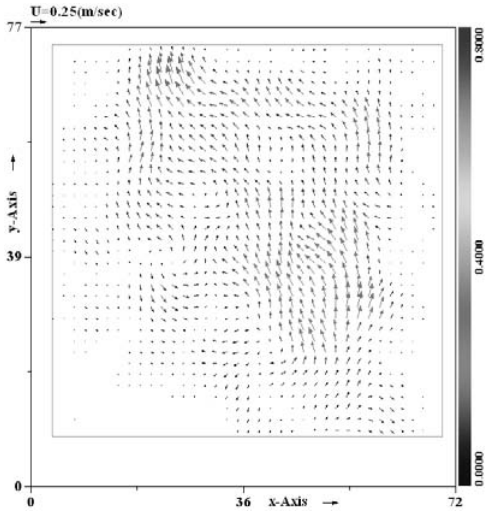

Fig. 11. Velocity vectors showing the low air velocity during the transition period at f = 0.9 Hz for D = 260 mm.

Table 1. Kinetic energy of the air in the turbine chamber.

Location	Max. K.E. (J/kg)	Min. K.E. (J/kg)	Avg. K.E. (J/kg)
Top (●)	0.435	0.000052	0.03
Middle(●)	0.291	0.00025	0.028
Bottom (●)	0.134	0.000004	0.015

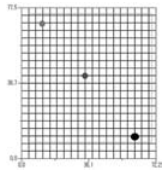

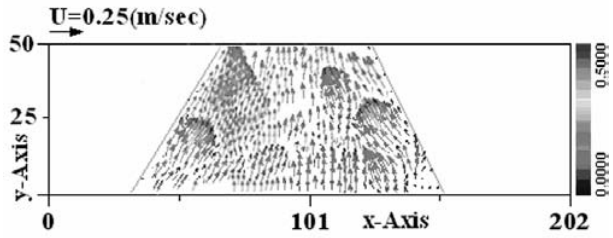

Fig. 12. Velocity vectors in the contraction before the turbine chamber at f = 0.9 Hz and D = 260 mm.

Figs. 7 and 8.

It was observed that there is a period of low air velocities in both the upward and downward directions; this happens when the free surface of the water in the OWC is stationary for a while before changing its direction of oscillation. Fig. 11 shows the velocity vectors at such an instant. While fluctuating vertical velocities and forces were also reported by Conde and Gato [14] from their numerical work, the fluctuations in the *v*-component of velocity were symmetric about the mean velocity (equal inward and outward flow velocities). The present results clearly prove that the upward and downward flows are not similar. Setoguchi et al. [25] also reported that in full scale OWCs, the velocity is higher when the air flows out to the atmosphere (exhalation) than in the reverse direction.

An OWC is a wave-breaking device; when the wave impinges, the upper surface of the water in the OWC is free to move upwards, hence it will exert more pressure on the air compared to when the wave recedes when the water movement downwards is blocked by the water that is accumulated near the OWC. Most of the turbines for OWC applications are designed with the assumption of equal velocities in both the flow directions; this may lead to poor performance of the turbine.

The velocity vectors in the air chamber before the turbine chamber are shown in Fig. 12. It can be seen that the velocities in this case are lower compared to those in the turbine chamber (Fig. 9). The flow is accelerating inside the converging section. However, the nozzle-effect provided by the specially designed air chamber causes the flow to accelerate inside the turbine chamber, as described earlier. The air velocities at the entrance to the turbine chamber were found to be the highest for the frequency of 0.9 Hz and the distribution was quite uniform across the width of the chamber, which is clear from Fig. 12.

The kinetic energy of the air was calculated from PIV measurements of instantaneous velocities with the relation

$$K.E. = \frac{1}{2}(u^2 + v^2) \tag{1}$$

From these data, the maximum, average and minimum kinetic energies of the air in the turbine chamber were obtained at three locations. Table 1 shows these values. It can be seen that the maximum K.E. is higher at the top location, where the average K.E. is also found to be the highest compared to the middle and bottom locations. It is also interesting to see that the minimum K.E. is very small compared to the average K.E. at all these locations. Similar results are presented by Lin and Dorrell [20] who showed that the power available to the turbine varies by nearly 100% during a given airflow cycle. There have been attempts to solve the problems of excessively high air velocities and the associated drop in the performance of the turbines due to stalling of the turbine blades by changing the pitch of the blades or by providing relief valves to control the airflow rate [15].

The present results highlight the need to regulate the flow of air into the turbine. It is felt that an airflow regulator provided in series with the turbine would be more useful than a relief valve that only reduces the excessive pressure. Although it was reported earlier [15] that the valve provided in series with the turbine increases the pressure oscillations, it is felt that it would ensure a relatively steady flow of air into the turbine. A Savonius turbine in such a rectangular OWC with an innovative contraction design is expected to perform much better compared to the conventional turbines used in circular OWC systems. It is also quite easy to increase the width of the capture chamber in practical systems and extract more power from the waves by employing either a large rotor or a number of rotors in segments; this is not possible in circular OWC systems.

4. Conclusions

The airflow in the OWC chamber was studied with the help of pressure and velocity measurements. The air velocities in the turbine chamber during the upward motion of water as a result of wave impingement in the column are always larger than those during the downward motion. The oscillating pressures in the air chamber agree well with the fluctuating velocities recorded with PIV measurements. The contraction design before the turbine chamber ensured a well-directed flow in the chamber that will impart considerable momentum to the blades of the turbine. While the airflow was strong most of the time, low air velocities were recorded during the transition between the downward and upward flows when the free surface of the water in the OWC is stationary for a while before changing its direction of oscillation, indicating the need of a flow regulator.

Nomenclature

D : Water depth, m
f : Wave frequency, Hz
H : Wave height, m
L : Wavelength, m
u : Horizontal component of velocity, m/s
v : Vertical (streamwise) component of velocity, m/s
x : Horizontal (transverse) coordinate, m
y : Vertical (streamwise) coordinate, m

References

[1] J. Falnes, A review of wave-energy extraction, *Marine Structures*, 20 (4) (2007) 185-201.

[2] M. E. McCormick, Ocean wave energy conversion, first ed., Dover Publications, New York, USA, 7-14 (2007) 45-136.

[3] R. G. Dean and R. A. Dalrymple, Water Wave Mechanics for Engineers and Scientists, World Scientific Publishing Co., Singapore, (1991) 41-123.

[4] G. L. Pickard and S. Pond, Introductory Dynamical Oceanography, Butterworth-Heinemann, Oxford (1986) 207-231.

[5] L. H. Holthuijsen, Waves in oceanic and coastal waters, *Cambridge University Press*, United Kingdom (2007) 118-132.

[6] B.LeMéhauté, An Introduction to Hydrodynamics and Water Waves, Springer-Verlag, New York, USA (1976) 197-255.

[7] C. Gray and C. A. Greated, The application of particle image velocimetry to the study of water waves, *Optics and Lasers in Engineering*, 9 (3-4) (1988) 265-276.

[8] D. Stagonas and G. Müller, Wave field mapping with particle image velocimetry, *Ocean Engineering*, 34 (11-12) (2007) 1781-1785.

[9] M. Raffel, C. Willert and J. Kompenhans, Particle Image Velocimetry – *A Practical Guide, first ed*., Springer, Berlin Heidelberg, Germany, (1998) 105-166.

[10] R. Pelc and R. M. Fujita, Renewable energy from the ocean, *Marine Policy*, 26 (6) (2002) 471-479.

[11] D. V. Evans and R. Porter, Hydrodynamic characteristics of an oscillating water column device, *Applied Ocean Research*, 17 (3) (1995) 155-164.

[12] Y. M. C. Delauré and A. Lewis, 3D hydrodynamic modelling of fixed oscillating water column wave power plant by a boundary elements methods, *Ocean Engineering*, 30 (3) (2003) 309-330.

[13] C. Josset and A. H. Clément, A time-domain numerical simulator for oscillating water column wave power plants, *Renewable Energy*, 32 (8) (2007) 1379-1402.

[14] J. M. Paixão Conde and L. M. C. Gato, Numerical study of the air-flow in an oscillating water column wave energy converter, *Renewable Energy*, 33 (12) (2008) 2637-2644.

[15] A. F. de O. Falcão and P. A. P. Justino, OWC wave energy devices with air flow control, *Ocean Engineering*, 26 (12) (1999) 1275-1295.

[16] A. J. N. A. Sarmento, Wave flume experiments on two-dimensional oscillating water column wave energy devices, *Experiments in Fluids*, 12 (4-5) (1992) 286-292.

[17] P. M. Koola, M. Ravindran and P. A. A. Narayana, Model studies of oscillating water column wave-energy device, *ASCE Journal of Energy Engineering*, 121 (1) (1995) 14-26.

[18] T. Setoguchi, S. Santhakumar, H. Maeda, M. Takao and K. Kaneko, A review of impulse turbines for wave energy conversion, *Renewable Energy*, 23 (2) (2001) 261-292.

[19] D. G. Dorrell and W. Fillet, Investigation of a small-scale segmented oscillating water column utilizing a Savonius rotor turbine, *Proceedings of the International Conference on Energy and Environment (ICEE 2006) held in Selangor*, Malaysia, 23-32.

[20] C. C. Lin and D. G. Dorrell, A small segmented oscillating water column using a Savonius rotor turbine, *Proceedings of IEEE International Conference on Sustainable Energy Technologies (ICSET 2008) held in Singapore*, 508-513.

[21] J. -L Menet, A double-step Savonius rotor for local production of electricity, *Renewable Energy*, 29 (2004) 1843-1862.

[22] B. D. Altan and M. Atılgan, The use of a curtain design to increase the performance level of a Savonius wind rotors, *Renewable Energy*, 35 (2010) 821-892.

[23] T. Setoguchi and M. Takao, Current status of self rectifying air turbines for wave energy conversion, *Energy Conversion and Management*, 47 (2006) 2382-2396.

[24] M. Rea, Wave tank and wavemaker design, in Ocean wave energy – current status and future perspectives, ed. João Cruz, Springer-Verlag, Berlin Heidelberg, Germany, (2008) 147-159.

[25] T. Setoguchi, S. Santhakumar, M. Takao, T. H. Kim and K. Kaneko, A modified wells turbine for wave energy conversion, *Renewable Energy*, 28 (2003) 79-91.

Krishnil Ravinesh Ram obtained his BETech degree in Mechanical Engineering from The University of the South Pacific (USP) in 2007. He is pursuing his post-graduate studies and is also employed at USP as a Tutor in Mechanical Engineering. He is currently involved in research work in the area of ocean wave energy.

Young-Ho Lee obtained his Ph.D. degree from the Department of Mechanical Engineering, University of Tokyo, Japan, in 1992. Currently, he is a professor in the Division of Mechanical Engineering at the Korea Maritime University. He is the vice president of Korea Wind Energy Association and Korea Fluid Machinery Association.